ELSEVIER

Journal of Fluids and Structures 21 (2005) 531–542

JOURNAL OF FLUIDS AND STRUCTURES

www.elsevier.com/locate/jfs

A reduced order system ID approach to the modelling of nonlinear structural behavior in aeroelasticity

P.J. Attar[a,*], E.H. Dowell[b,1]

[a]*Air Force Research Laboratory, AFRL/VAAC, 2210 Eighth St., Bldg 146, WPAFB,OH 45433-7512, USA*
[b]*Pratt School of Engineering, Box 90300, Duke University, Durham NC 27708, USA*

Received 20 April 2005; accepted 11 August 2005

Abstract

A method is proposed for identifying a set of reduced order, nonlinear equations which describe the structural behavior of aeroelastic configurations. The strain energy of the system is written as a (polynomial) function of the structures' modal amplitudes. The unknown coefficients of these polynomials are then computed using the strain energy data calculated from a steady state, high-order, nonlinear finite element model. The resulting strain energy expression can then be used to develop the modal equations of motion. From these equations, zero and nonzero angle of attack flutter and limit cycle oscillation data are computed for a 45° delta wing aeroelastic model. The results computed using the reduced order model compare well with those from a high-fidelity aeroelastic model and to experiment. A two to three order of magnitude reduction in the number of structural equations and a two order of magnitude reduction in total computational time is accomplished using the current reduced order method.

Keywords: Nonlinear aeroelasticity; System identification

1. Introduction

In recent years various reduced order methods have been developed and used in the field of aeroelasticity. Normal mode reduced order modal methods, which have been used in the field of structural dynamics for many years, have now also been applied to obtain reduced order aerodynamic models (Dowell, 1996; Hall, 1994; Tang et al., 1999). In cases where the computation of the normal modes of the structural or aerodynamic system becomes too computationally expensive, methods such as the proper orthogonal decomposition technique (POD), which extract dynamic information from time domain or frequency domain computations, have been utilized (Epureanu et al., 2000, 2001; Hall et al., 1999; Romanowski, 1996). Also Hall and his colleagues have recently developed another novel technique which uses a harmonic balance solution for a set of nonlinear ordinary equations in time. This method has been used to compute solutions to nonlinear computational fluid dynamics (CFD) problems (Hall et al., 2002; Thomas et al., 2002, 2004; Kholodar et al., 2002).

*Corresponding author. Tel.: +1 937 255 0057; fax: +1 937 656 7857.
E-mail addresses: peter.attar@wpafb.af.mil (P.J. Attar), dowell@ee.duke.edu (E.H. Dowell).
[1]William Holland Hall Professor, Department of Mechanical Engineering and Materials Science, Director of the Center for Nonlinear and Complex Systems and Dean Emeritus, Duke University.

0889-9746/$ - see front matter
doi:10.1016/j.jfluidstructs.2005.08.012

Nomenclature

$\boldsymbol{A_b}$	matrix of aerodynamic bound circulation influence coefficients
$\boldsymbol{A_w}$	matrix of aerodynamic wake circulation influence coefficients
$A_{ijkl\cdots o}$, A_i	polynomial coefficients in strain energy expression
$\boldsymbol{C}$	structural damping matrix
$\boldsymbol{E}$	matrix of interpolation coefficients
$\boldsymbol{F}^P$	vector of structural nodal forces due to applied pressure
$\boldsymbol{F}^{SE}$	vector of structural nodal forces derived from a strain energy function
$\tilde{\boldsymbol{F}}^{SE}$	vector of structural modal forces derived from a strain energy function
$\boldsymbol{M}$	structural mass matrix
$\boldsymbol{M}_i$	largest power to which ith modal amplitude is raised to in strain energy expression
$\boldsymbol{N}$	number of structural modes kept in modal expansion
$\boldsymbol{n}$	discrete time level in aerodynamic equations of motion
$\boldsymbol{N}_t$	number of terms in strain energy expression
$\boldsymbol{N}_{\text{full}}$	number of degrees of freedom in finite element model
$\boldsymbol{q}$	vector of structural modal amplitudes
U	strain energy function
$\boldsymbol{u}_z$	vector of out-of-plane nodal degrees of freedom
$\boldsymbol{u}$	vector of structural nodal degrees of freedom
$\boldsymbol{\alpha}$	wing angle of attack
$\boldsymbol{\Gamma_b}$	vector of aerodynamic bound circulation
$\boldsymbol{\Gamma_w}$	vector of aerodynamic wake circulation
$\boldsymbol{\Phi}$	matrix of structural modal vectors
$\boldsymbol{\phi}_i$	ith structural modal vector
$\psi_i(q_1, q_2, \ldots, q_N)$	the ith polynomial basis function in the strain energy expression

A disadvantage of the methods used in the above studies is that the original full order equations of motion must be available to construct the reduced order model. If, for example, the engineer wants to construct a reduced order model for a system which was initially modelled using a commercial package, then most often this approach will not be viable since the actual equations are not available to the user. Worst yet, the situation could be that the engineer has data which was taken experimentally and for which a theoretical model has not been constructed. In these cases a method must be used which can take output and/or input data from a "black box" source and construct a reduced set of equations which can be used as a predictive tool. These methods are often called system identification techniques.

In the field of structural dynamics, a large amount of research exists on identifying the parameters for linear systems. Juang (1994) and Juang and Pappa (1985) have developed techniques which are able to take input and output data and construct the system modal damping and frequencies. These same methods were used to determine the controllability of aerodynamic modes in a linear vortex lattice aerodynamic model (Tang et al., 2001; Kim, 2004). However the methods used in the work by Juang and Pappa (1985) and Kim (2004) will only be valid if the considered system can be assumed to be behaving in a linear manner.

In recent years some work has been done in the area of nonlinear system identification. In recent work by Epureanu and Dowell (2003), a multivariate, third order polynomial was used as the functional form for a nonlinear structural model used in the computation of panel limit cycle oscillations (LCO). Time series data from a finite difference solution of the original nonlinear equations was used to identify the coefficients of the polynomial. Gabbay et al. (2000) and Mehner et al. (2000) used polynomial functions whose coefficients were identified using strain energy data from a series of finite element runs, to model a microelectromechanical system. Silva et al. have used a Volterra series approach to identify linear and nonlinear aerodynamic systems (Silva, 1997, 1999; Silva and Raveh, 2001; Silva and Bartels, 2002; Lucia et al., 2003). Denegri and Johnson (2001) have conducted a study based upon a neural network model using flight test data which has shown promise. Lucia et al. (2004) have prepared a comprehensive review of reduced order modelling methods including those based upon system identification.

In the work to be presented here, the LCO of a 45° delta wing will be computed using a linear vortex lattice model which is coupled to a nonlinear structural model. The structural model used here is constructed by a nonlinear system identification of a high-fidelity nonlinear finite element model. Flutter and LCO results are presented for zero and nonzero angles of attack. The results from this model are compared to results for two different theoretical models and to experimental results.

2. Theory

2.1. Full aeroelastic equations

In the work to be presented in this paper, the nonlinear aeroelastic model consists of a linear vortex lattice aerodynamic model coupled to a nonlinear structural model. Only an abbreviated discussion of the full order system of

aeroelastic equations will be presented here. For a more detailed discussion of these equations please see the work by Attar et al. (2003, 2004b). Note that in the following text, boldface quantities denote vector quantities.

The general form of the aeroelastic system of equations, using a finite element solution of the structural equations, can be written in the following manner:

$$\boldsymbol{M}\ddot{\boldsymbol{u}} + \boldsymbol{C}\dot{\boldsymbol{u}} + \boldsymbol{F}^{SE} = \boldsymbol{F}^{P}, \tag{1}$$

$$\boldsymbol{A}_{\boldsymbol{b}}\boldsymbol{\Gamma}_{\boldsymbol{b}}^{n+1} = \boldsymbol{E}\,\frac{\partial \boldsymbol{u}_z^{n+1/2}}{\partial t} + \boldsymbol{E}\,\frac{\partial \boldsymbol{u}_z^{n+1/2}}{\partial x} + \boldsymbol{\alpha} - \boldsymbol{A}_{\boldsymbol{w}}\boldsymbol{\Gamma}_{\boldsymbol{w}}^{n}, \tag{2}$$

where in the structural equations of motion, Eq. (1), the vector $\boldsymbol{u}$ contains the structural nodal degrees of freedom, the matrix $\boldsymbol{M}$ is the mass matrix, $\boldsymbol{C}$ is the damping matrix and $\boldsymbol{F}^{P}$ is the load vector due to the aerodynamic pressure. The vector $\boldsymbol{F}^{SE}$ is a vector of forces due to the strain energy of the system and is written as

$$\boldsymbol{F}_i^{SE} = \frac{\partial U}{\partial u_i}, \tag{3}$$

where U is the strain energy functional for the system. In the aerodynamic equations of motion, Eq. (2), $\boldsymbol{\Gamma}_{\boldsymbol{b}}$ and $\boldsymbol{\Gamma}_{\boldsymbol{w}}$ are vectors of wing and wake circulations, respectively, the matrices $\boldsymbol{A}_{\boldsymbol{b}}$ and $\boldsymbol{A}_{\boldsymbol{w}}$ are the wing and wake influence coefficient matrices and the matrix $\boldsymbol{E}$ is a matrix of interpolation coefficients needed to transfer quantities from the finite element mesh to the aerodynamic mesh. The vector $\boldsymbol{u}_z$ is the out-of-plane degree of freedom at each of the aerodynamic collocation points. Also the vector $\boldsymbol{\alpha}$ contains the (constant) angle that the wing root chord makes with the freestream flow and the superscript n refers to a time-step value in the time integration of the equations. The aerodynamic pressure used in Eq. (1) is found by combining the solution of Eq. (2) with the linearized Bernoulli equation.

Eqs. (1) and (2) are coupled through the $\boldsymbol{F}^{P}$ term in Eq. (1) and through the terms involving $\boldsymbol{u}_z$ in Eq. (2). Implicit coupling of these two equations is accomplished using a global subiteration technique. During each subiteration the aerodynamic forces on the structure are updated and the resulting deflections are then passed back to the aerodynamic solver. In order to proceed to the next timestep convergence must be achieved for successive subiteration values of the quantities (pressure, displacement and velocity) passed back and forth to the two solvers.

While the above set of equations and solution procedure give very accurate results for aeroelastic problems which exhibit large deflections and rotations (Attar et al., 2004b), the computational time can be prohibitively large, often requiring days to simulate a few seconds of system response. The reason for this is that Eq. (1) is a nonlinear equation with a moderate to large number of degrees of freedom (10^3–10^5) and the solution of this nonlinear equation often requires several Newton–Raphson iterations within each subiteration. In the next two sections a method will be described which is able to reduce the size of Eq. (1) by 10^2–10^4 degrees of freedom and in the process decrease the solution time dramatically while maintaining good accuracy.

2.2. Reduced order aeroelastic equations

The use of the normal modes of a structure to reduce the dimensionality of large, linear finite element models is a common practice and proves to be an effective means of reducing simulation times. The use of normal modes allows a model to retain the important dynamic characteristics while producing a much more compact and lower dimensional system of equations. However, the use of normal modes has been less commonplace in cases where structural nonlinearities are to be included in a finite element analysis. In this section a reduced order nonlinear structural model is developed that expresses the strain energy functional, U, as a polynomial in the modal coordinates of the structure. The coefficients of this polynomial will be determined using modal and strain energy information computed using a high-fidelity, finite element model.

The general form of Eq. (1) written in terms of modal coordinates can be expressed in the following manner:

$$\boldsymbol{\Phi}^{\mathrm{T}}\boldsymbol{M}\boldsymbol{\Phi}\ddot{\boldsymbol{q}} + \boldsymbol{\Phi}^{\mathrm{T}}\boldsymbol{C}\boldsymbol{\Phi}\dot{\boldsymbol{q}} + \tilde{\boldsymbol{F}}^{SE}(\boldsymbol{q}) = \boldsymbol{\Phi}^{\mathrm{T}}\boldsymbol{F}^{P}, \tag{4}$$

where the nodal degrees of freedom are expressed as a linear combination of the modes,

$$\boldsymbol{u} = \sum_{i=1}^{N_{\mathrm{full}}} q_i(t)\boldsymbol{\phi}_i, \tag{5}$$

and the matrix $\boldsymbol{\Phi}$ contains the mode shape vectors $\boldsymbol{\phi}_i$. Also, in Eq. (5), q_i is the ith modal degree of freedom and N_{full} is the total number of structural degrees of freedom in Eq. (1). Note that now the force vector due to strain energy, $\tilde{\boldsymbol{F}}^{SE}$, is a function of the modal amplitudes q_i. In practice the summation in Eq. (5) is truncated at N modal degrees of freedom

where N is a number much less than N_{full}. Likewise the aerodynamic equations of motion can now be expressed as

$$\boldsymbol{A}_b\boldsymbol{\Gamma}_b^{n+1} = \boldsymbol{E}\boldsymbol{\Phi}\dot{\boldsymbol{q}}^{n+1/2} + \boldsymbol{E}\boldsymbol{d}\boldsymbol{\Phi}\boldsymbol{q}^{n+1/2} + \boldsymbol{\alpha} - \boldsymbol{A}_w\boldsymbol{\Gamma}_w^n, \tag{6}$$

where the matrix $\boldsymbol{d\Phi}$ is the matrix of x derivatives of the modal functions.

One thing to note is that in Eqs. (4)–(6) the spatial modal vectors $\boldsymbol{\phi}_i$ do not have to be the normal modes of the system. If for some reason the normal modes cannot be found or are thought to not best represent the spatial complexity of the system, other modes (modes for example POD) can be used in place of the normal modes. Also in the work to be presented here, an assumption is made that only the modes in the out-of-plane direction need to be included in Eq. (5). However, this assumption is not a requirement for the method presented in this paper.

Now that the general form of the equations has been developed, a functional form for the strain energy U in terms of the modal coordinates q_i must be defined. Using classical continuum mechanics as a guide, a polynomial form for the strain energy functional is chosen. In this work a multivariate Lagrange polynomial is used. The form of this polynomial can be written in the following manner:

$$U = \sum_{i=0}^{M_1}\sum_{j=0}^{M_2}\sum_{k=0}^{M_3}\sum_{l=0}^{M_4}\cdots\sum_{o=0}^{M_N} A_{ijkl\ldots o}q_1^i q_2^j q_3^k q_4^l \ldots q_N^o = \sum_{i=1}^{N_t} A_i\psi_i(q_1, q_2, \ldots, q_N), \tag{7}$$

where the coefficients A_i are found using a least squares fit of strain energy data generated using a finite element package and the ψ_i are the Lagrange basis functions. The number of basis functions used, N_t, is the product of the values $M_1, M_2, \ldots, M_N$. The process of generating the data and finding the coefficients A_i will be explained in the next section. The values M_i in the summations of Eq. (7) represent the highest order polynomial kept for each individual mode. For example if M_1 is four, then the highest power that q_1 is raised to will be four.

Although the largest order univariate polynomial for the ith mode will be M_i, the polynomial order of Eq. (7) will be the sum of the M_i values. In the current work this leads to a polynomial which is of high order with some individual terms in Eq. (7) having orders greater than 16. This results in an ill-conditioned system of equations for the coefficients A_i. This is handled in the current work by employing a regularization method which uses a singular value decomposition to solve for the coefficients. Small singular values (small when compared to the largest) are neglected in the solution. Other reduced order polynomials could also be used which would reduce the ill-conditioning problems.

2.3. System identification procedure

In order to find the coefficients A_i in Eq. (7) the strain energy U must be computed for various out-of-plane spatial distributions $u_z(x, y)$. The structure is displaced to a static configuration $u_z^i(x, y)$ determined by the prescribed modal amplitudes q_j^i:

$$\boldsymbol{u}_z^i = \sum_{j=1}^{N} q_j^i\boldsymbol{\phi}_j. \tag{8}$$

The strain energy for this ith configuration, U^i, is then computed by solving a nonlinear statics problem. In the current work this was accomplished using the commercial finite element code ANSYS (ANSYS, 2002). Since the out-of-plane degrees of freedom $\boldsymbol{u}_z^i$ are pre-specified, the problem becomes one of determining the remaining degrees of freedom in the nodal degree of freedom vector $\boldsymbol{u}^i$. Once these are determined, they are then used, along with the specified out-of-plane degrees of freedom, to compute the strain energy for the ith configuration U^i.

Since the polynomials which are used in this work are higher order, and interpolation is usually a much more accurate process than extrapolation, it is important to properly choose the modal amplitude values. Determining what the range of the modal amplitude values should be in Eq. (8) can be accomplished in various ways. In this paper the range of the q_i's was determined using prior knowledge of the minimum and maximum values for these q_i's. If such knowledge is not available, one possible way of determining the range of q_i's would be to apply representative structural loads in the finite element model and solve for the displacement field. Using the linear modes of the structure a least squares problem could then be solved to determine the distribution of the q's which could then be used in generating the strain energy. Another method which could be used would be to give an absolute maximum and minimum value for q and then scale the individual modal values based upon their modal stiffness, ω_i^2.

Once each individual modal minimum and maximum has been determined, the number of values of the modal amplitudes between these two values should be determined. For example if 10 values are chosen for a particular mode, the structure strain energy would be computed for displacement fields which would contain 10 different modal values for that individual mode. The number of values chosen for a mode should be at least one higher than the highest order

polynomial (M_i) for that mode. This would seem to be a reasonable restriction since in order to be able to fit a nth order polynomial $n+1$ points must be given. For most problems in structural dynamics, the lower modes should have the most values since these modes most often dominate the response.

Once all of the strain energy values have been calculated using the finite element model, the coefficients in Eq. (7) can be computed using a least squares solution of the following set of linear equations:

$$\boldsymbol{A}\boldsymbol{x} = \boldsymbol{b}, \tag{9}$$

where the vector $\boldsymbol{b}$ contains the strain energy values for each individual configuration and the vector $\boldsymbol{x}$ contains the N_t polynomial coefficients. The Vandermonde matrix, $\boldsymbol{A}$, consists of the basis functions used in the polynomial expansion evaluated for each individual configuration and can be expressed as

$$\begin{bmatrix} \psi_1^1 & \psi_2^1 & \cdots & \psi_{N_t}^1 \\ \psi_1^2 & \psi_2^2 & \cdots & \psi_{N_t}^2 \\ \cdot & \cdot & \cdot & \cdot \\ \psi_1^{N_p} & \psi_2^{N_p} & \cdots & \psi_{N_t}^{N_p} \end{bmatrix}, \tag{10}$$

where the superscripts in Eq. (10) indicate the configuration number, the subscripts indicate the basis function number and N_p is the total number of strain energy calculations (configurations) which were performed. If $N_p \geqslant N_t$ then the system is of full rank and the least-squares solution of Eq. (9) is unique. If $N_p < N_t$, then there are an infinite number of solutions, and the one which minimizes the L2 norm of $\boldsymbol{x}$ is used. In the work which is discussed here, the value of N_p will be at least as large as N_t.

2.4. Overview of methodology

In this section an overview will be given of the steps needed to construct a nonlinear reduced order structural model using the system identification procedure described here.

Step 1: Construct, for the system which is to be investigated, a numerical discretization of the structural equations of motion. In this work the discretization was done using a finite element methodology, but finite difference or finite volume methods could also be used. If a certain element type is needed in order to include geometric nonlinearities, as is the case for some finite element codes, it needs to be included in this step.

Step 2: Compute representative spatial modes for the structure. In this work these modes were the normal modes computed by solving the linear eigenvalue problem. However, if these cannot be computed or are not the best modes for the problem, other spatial shape vectors such as Ritz vectors or POD modes can also be used.

Step 3: Decide which of the modes computed in step 2 are to be used in the reduced order model. In this work the first N modes are kept where the modes have only out-of-plane motion such as bending, torsion or both. If the in-plane displacement is needed modes which contain in-plane motion could also be included.

Step 4: Since the number of the nonlinear static solutions is tied to the order and type of polynomial which is being used to represent the strain energy functional, these decisions need to be made before the strain energy values are computed. In this work a multivariate Lagrange polynomial was used (form of the polynomial given in Eq. (7)). Also in this work for the first four modes kept in the model the highest order of each individual mode (M_i in Eq. (7)) was four while for modes higher than four the highest order for each mode was two.

Step 5: Choose the upper and lower limits for modal amplitude values to be used in the nonlinear static solutions. These can be chosen using prior experience or by applying representative loads to the model and computing the modal amplitudes using a least-squares method.

Step 6: Choose the number of values for each individual mode to be used in displacing the structure. For example, if for mode one (q_1) in step 5, maximum and minimum values of the modal amplitudes are chosen to be $-0.1 \leqslant q \leqslant 0.1$ and 11 values are chosen in this step, static displacements would be computed with values of q_1(along with whatever combinations are computed for the other modes) of: $-0.1, -0.08, -0.06, -0.04, -0.02, 0.00, 0.02, 0.04, 0.06, 0.08, 0.10$. In order that the least-squares solution for the coefficients in Eq. (7) is unique, the values chosen in this step should result in a total number of configurations (N_p) which is greater than or equal to the product of the M_i's in Eq. (7) (N_t).

Step 7: Displace the structure using a prescribed displacement based upon the values of the modal coordinates.

Step 8: Compute the strain energy for the final state of the model. The final state is found by solving a nonlinear static problem for the unknown degrees of freedom (i.e. all other displacements and rotations not fixed in step 7). In this work the unknown degrees of freedom are in-plane displacements (x and y displacement) and all rotations (rotation in x, y and z).

Step 9: Repeat steps 7 and 8 for all combinations of modal amplitudes as determined by steps 5 and 6.

Step 10: Solve a least-squares problem for the unknown coefficients in Eq. (7) using the strain energies computed in step 8 and the values of polynomial basis functions computed using the corresponding modal amplitudes used in step 7.

Step 11: Differentiate the strain energy polynomial with respect to each modal amplitude and combine this with the corresponding modal inertia and damping terms in order to construct the nonlinear modal equations of motion (Eq. (4)).

Step 12: Combine Eq. (4) with a suitable fluid model in order to obtain a nonlinear, time dependent aeroelastic system of equations.

3. Results

In the work presented here a thin plate, 45° delta wing is modelled. The wing is constructed of a plexiglas material and has a constant thickness of 0.0016 m. The trailing edge span dimension of the wing is 0.381 m and the root chord dimension is 0.381 m. The wing is clamped along the middle 60% of root chord. In this work all of the structural degrees of freedom are constrained along this partial clamp.

The results shown below for the high-fidelity method, labelled ANSYS in the figures, are taken from the work of Attar et al. (2004b). The aerodynamic model used in that work is identical to the one used here. The structural model is the same one which is used to compute the strain energy in the current reduced order methodology. The model contained 552 shell elements with 614 nodes for a total of 3684 degrees of freedom. Structural nonlinearities modelled included large rotation (using a co-rotational formulation) and stress-stiffening.

Results will also be presented for an aeroelastic model which uses a reduced order von Karman structural model. The von Karman plate model is a classical method used to model geometric nonlinearities in thin-plates. However, as was discussed in Attar et al. (2004a) for problems where rotations are moderate, and any out-of-plane loading is expected to be handled predominantly by bending stiffness (such as a cantilever plate problem), the von Karman model performs poorly. The reduced order von Karman results shown below use 10 out-of-plane modes and 100 in-plane modes. Flutter and LCO results computed by the von Karman model for nonzero angle of attack are not presented in the figures below. This is due to the large inaccuracy of the results (flutter speeds of 36 and 57 m/s for $\alpha = 1$ and $\alpha = 2$) and the observation that including them skews (in a favorable manner!!) the appearance of the system identification model results.

In the reduced order, system identification results presented below, the values used for the M_i in Eq. (7) are:

$$M_i = 4, \quad i <= 4,$$
$$M_i = 2, \quad i > 4.$$

It was determined that using values of M_i larger than four for the first 4 modes did not have an effect on the solution. This was also the determination made for values larger than two for modes greater than the fourth.

The number of individual values for each of the modes used in the generation of strain energy was (mode 1 to mode 7): 7,5,5,5,3,3,3. Therefore, in the results shown below, if the computation is said to have used four modes $7 \times 5 \times 5 \times 5 = 875$ different configurations would be used to generate the strain energy function. Note that the number of configurations increases dramatically as the number of modes used increases. However, the static computations can be run in parallel which can help to relieve the computational burden of this preprocessing step. Also "design of experiment" type methods such as central composite design (CCD) (Myers and Montgomery, 2002) may be used to reduce the number of total data points used to fit the strain energy function.

Fig. 1 shows the static tip deflection of the delta wing at a flow velocity below the flutter speed (21 m/s) as a function of angle of attack. It appears that, when compared to the reduced order von Karman model, the current method produced results which are much closer to those computed using the high-fidelity model. Also, as the number of modes used in the model are increased, the results seem to be converging towards the ANSYS model results. This is shown more clearly in Fig. 2 which is a plot of the fractional error in the static deflection as predicted by the current reduced order model. The high-fidelity model results are used as the baseline results with which the error was computed.

Figs. 3 and 4 are plots of the flutter speed and flutter frequency of the delta wing model as a function of angle of attack. Along with the current system identification results, data is shown for both the high-fidelity aeroelastic model and experiment. Once again the system identification results are presented for various numbers of modes used in the computation. For angles of attack of less than 4°, the system identification model does a good job of predicting both the flutter speed and frequency when seven modes are included. Generally the lower the angle of attack, the fewer the number of modes that are needed to predict accurately the flutter parameters. The same can be said for the prediction of

static deflection shown in Fig. 1. However, if Figs. 3 and 4 are examined closely, one will note that unlike Figs. 1 and 2 where the change in the predicted static deflection appears to be a fairly smooth, monotonic function of the number of modes used, the flutter velocity and flutter frequency curves are not. This is especially true for angles of attack greater than 1° and less than 4°. For these cases the inclusion of the seventh mode appears to have a dramatic effect on both the predicted flutter speed and frequency. This is shown more clearly in Figs. 5 and 6, which are plots of the fraction error (when compared to the high-fidelity model) in the computed flutter speed and frequency as a function of number of modes kept in the model. Also note that, for the 4° angle of attack case, it is apparent that more than seven modes are necessary for an accurate solution. Here it is emphasized that the flutter velocity for nonzero angle of attack depends upon the nonlinearities in the structural model.

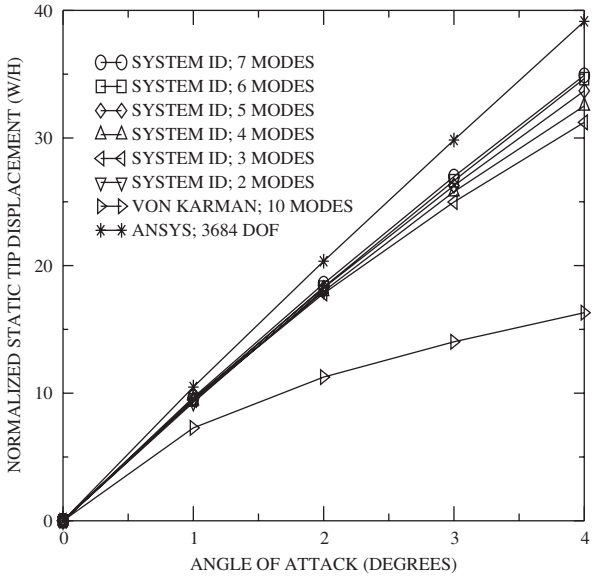

Fig. 1. Delta wing static tip deflection versus angle of attack at a flow velocity of 21 m/s.

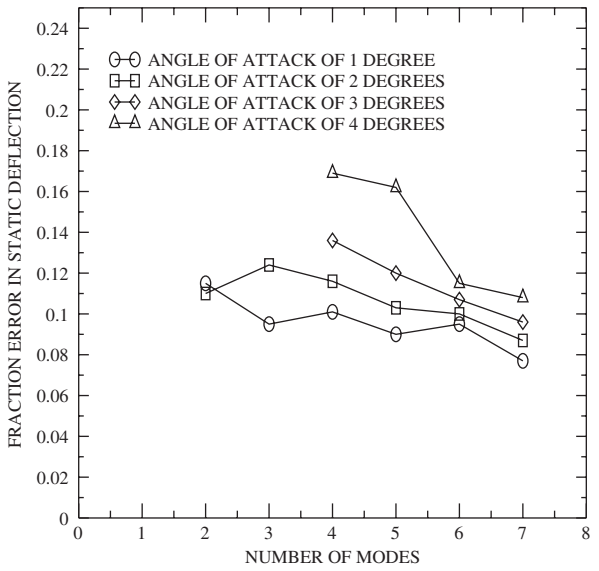

Fig. 2. Fractional error in the prediction of the static deflection computed using the reduced order model.

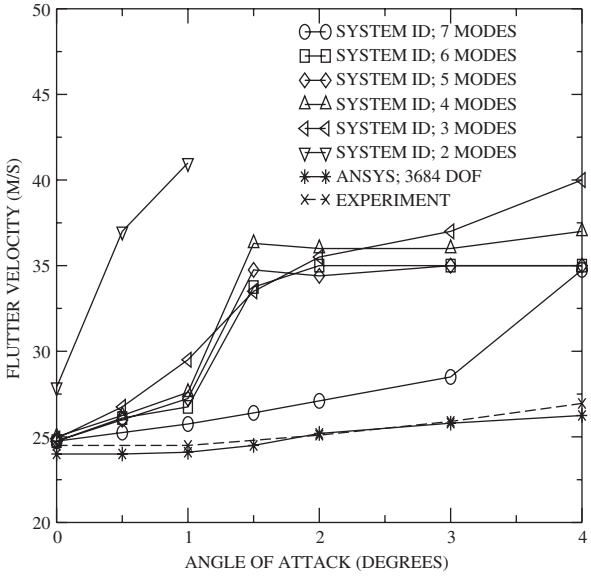

Fig. 3. Delta wing flutter velocity plotted as a function of angle of attack.

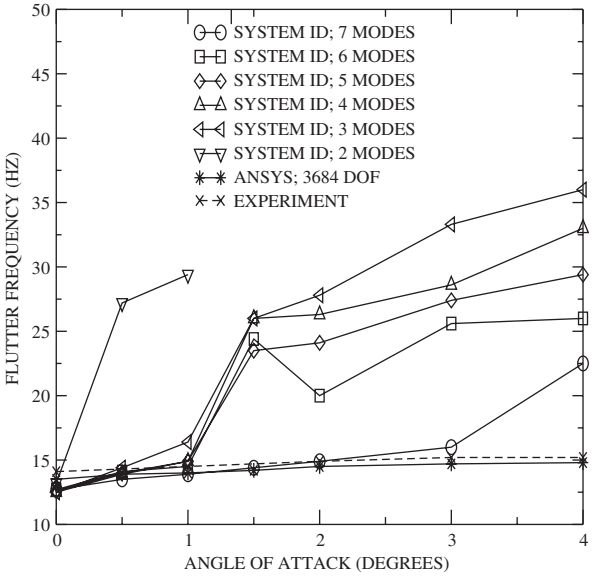

Fig. 4. Delta wing flutter frequency plotted as a function of angle of attack.

The magnitude of the Delta wing LCO tip velocity is shown in Figs. 7–9 for angles of attack of 0°, 1° and 2°. Only results for the system identification model with seven modes are included in the figures. The system identification model results are comparable to those obtained using the aeroelastic model which used the high-fidelity structural model. They are also in good agreement with experiment. As the angle of attack increases, and the flutter point accuracy decreases (as seen in Fig. 3), the quantitative accuracy of the current model decreases. However, qualitatively the behavior of the current model is very similar to that of the high-fidelity model for the results for all of the angles of attack presented. This is a good indicator that the nonlinear behavior (or lack thereof) of the high-fidelity model is being captured

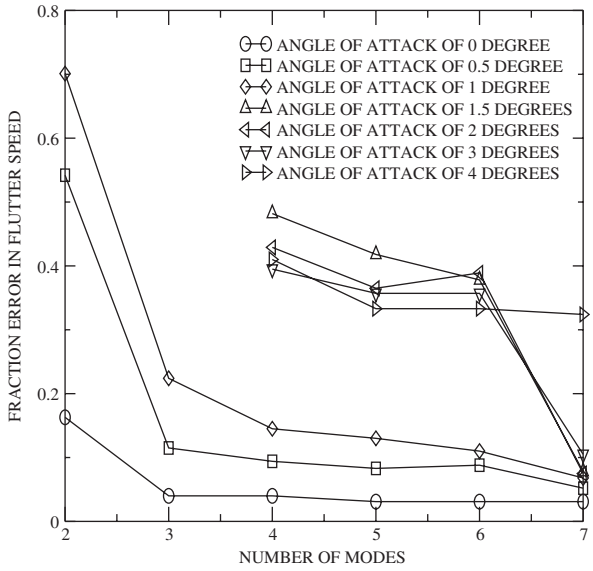

Fig. 5. Fractional error in the flutter velocity predicted using the reduced order model.

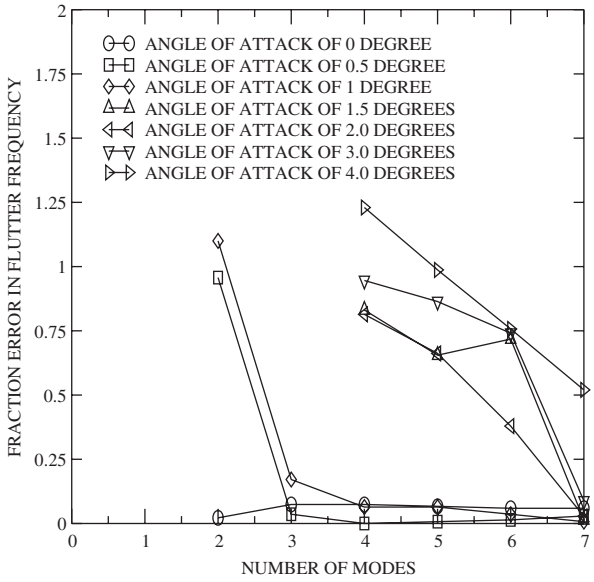

Fig. 6. Fractional error in the flutter frequency predicted using the reduced order model.

accurately by the reduced order system identification model. This is different than the LCO results presented for the von Karman model at zero angle of attack in Fig. 7. Even when 10 out-of-plane modes are used (the same modes which are used in the current reduced order model) the von Karman results are poor. As was mentioned previously in this section, nonzero angle of attack results are not plotted here for the von Karman model due to the large error in these results.

The preprocessing overhead increases by at least threefold (the increase depends on the value of M_i for the added mode) every time an additional mode is added to the system identification model. However, once this overhead is incurred, no additional computational resources are spent building the model. In the above examples the number of equations used to describe the structural motion was at most seven, which is three orders of magnitude less than the number of equations used in the nonlinear finite element model.

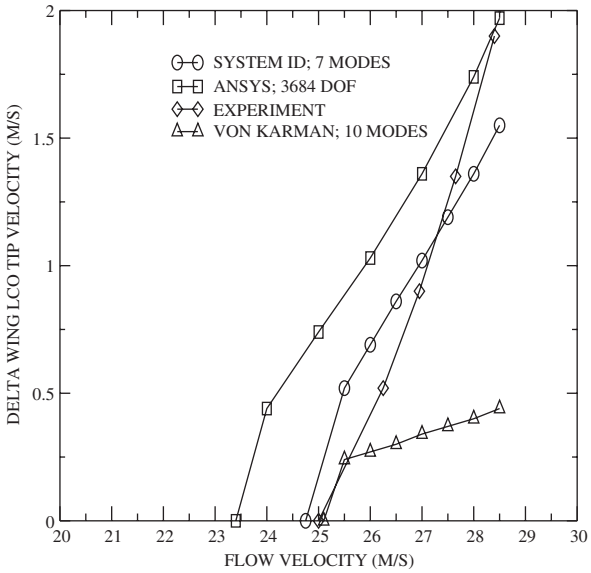

Fig. 7. Delta wing LCO tip velocity at 0° angle of attack plotted versus flow velocity.

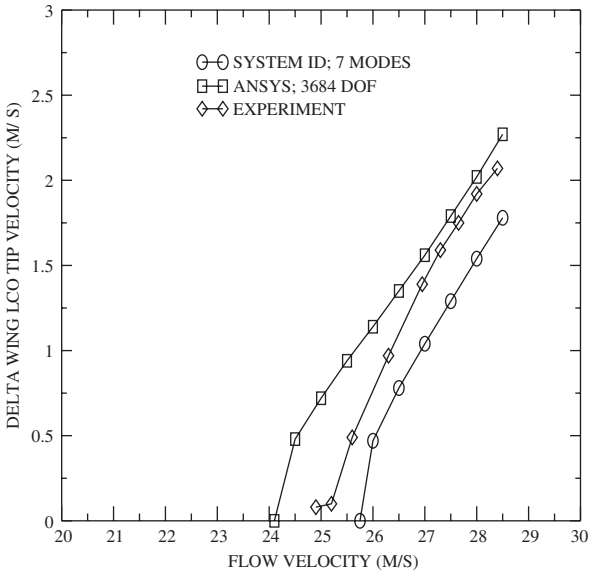

Fig. 8. Delta wing LCO tip velocity at 1° angle of attack plotted versus flow velocity.

4. Concluding remarks

A system identification methodology was presented for the reduced order modelling of nonlinear structural behavior in aeroelastic configurations. The idea is to write the strain energy as a function of the structure's modal amplitudes. The unknown coefficients in the strain energy function are then computed using data calculated using a high-order finite element model. This strain energy can then be differentiated with respect to the modal amplitudes to obtain the force on the structure due to stiffness in the equations of motion.

The flutter and LCO results from this model are computed for zero and nonzero angle of attacks and compare favorably with results calculated using an aeroelastic model with a nonlinear finite element structural model. It was

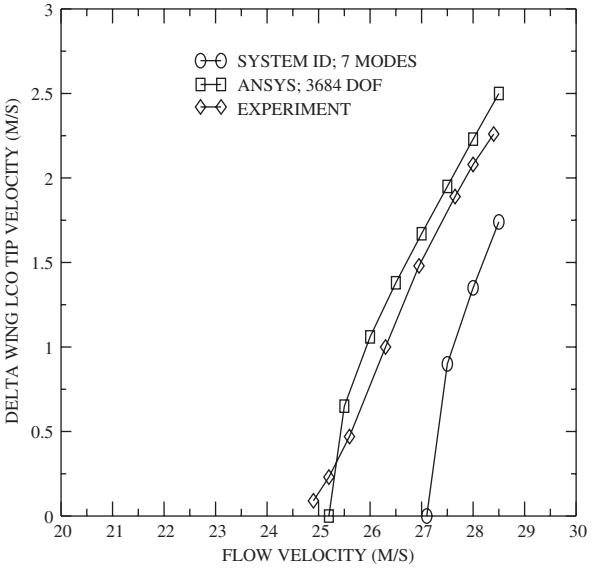

Fig. 9. Delta wing LCO tip velocity at 2° angle of attack plotted versus flow velocity.

found, not surprisingly, that, as the angle of attack is increased, more modes are needed to give accurate predicted flutter parameters. The addition of the seventh mode results in a dramatic improvement in the accuracy of the system identification model for angles of attack greater than 1°.

While the computation of the strain energy function does increase the preprocessing computational time, a three orders of magnitude reduction in the number of structural equations is realized using the current reduced order methodology. This resulted in a two orders of magnitude reduction in total computational time.

Acknowledgements

This work was funded in part by AFOSR grant "A Study of Uncertainty in Aeroelastic Systems", Captain and Dr Clark Allred is the program director.

References

ANSYS, 2002. ANSYS User Manual, Release 7.1. Swanson Analysis Systems, Inc.

Attar, P., Dowell, E., Tang, D., 2003. Theoretical and experimental investigation of the effects of a steady angle of attack on the nonlinear flutter of a delta wing plate model. Journal of Fluids and Structures 17, 243–259.

Attar, P., Dowell, E., White, J., 2004a. Modeling the LCO of a delta wing using a high fidelity structural model. Journal of Aircraft 42 (5), 1209–1217.

Attar, P., Dowell, E., White, J., 2004b. Modeling the LCO of a delta wing using a high fidelity structural model, AIAA Paper 2004-1402.

Denegri, C., Johnson, M., 2001. Limit cycle oscillation prediction using artificial neural networks. Journal of Guidance, Control and Dynamics 24 (5), 887–895.

Dowell, E., 1996. Eigenmode analysis in unsteady aerodynamics: reduced order models. AIAA Journal 34 (8), 1578–1588.

Epureanu, B.I., Dowell, E.H., 2003. Compact methodology for computing limit-cycle oscillations in aeroelasticity. Journal of Aircraft 40 (5), 955–963.

Epureanu, B., Dowell, E., Hall, K., 2000. Reduced-order models of unsteady transonic viscous flows in turbomachinery. Journal of Fluids and Structures 14, 1215–1234.

Epureanu, B., Hall, K., Dowell, E., 2001. Reduced-order models of unsteady viscous flows in turbomachinery using viscous-inviscid coupling. Journal of Fluids and Structures 15, 255–276.

Gabbay, L.D., Mehner, J.E., Senturia, S.D., 2000. Computer-aided generation of nonlinear reduced-order dynamic macromodels—I: Non-stress-stiffened case. Journal of Microelectromechanical Systems 9 (2), 262–269.

Hall, K., 1994. Eigenanalysis of unsteady flows about airfoils, cascades and wings. AIAA Journal 32 (12), 2426–2432.
Hall, K., Thomas, J., Dowell, E., 1999. Reduced-order modeling of unsteady small-disturbance flows using a frequency-domain proper orthogonal decomposition technique, AIAA Paper 99-0655.
Hall, K., Thomas, J., Clark, W., 2002. Computation of unsteady nonlinear flows in cascades using a harmonic balance technique. AIAA Journal 40 (5), 879–886.
Juang, J.-N., 1994. Applied System Identification. Prentice-Hall, Englewood Cliffs.
Juang, J.-N., Pappa, R., 1985. An eigensystem realization algorithm for modal parameter identification and model reduction. Journal of Guidance, Control, and Dynamics 8, 620–627.
Kholodar, D.B., Thomas, J.P., Dowell, E.H., Hall, K.C., 2002. A parametric study of transonic airfoil flutter and limit cycle oscillation behavior, AIAA Paper 2002-1211.
Kim, T., 2004. An efficient model reduction method for linear dynamics systems with multiple inputs, AIAA Paper 2004-2036.
Lucia, D., Beran, P., Silva, W., 2003. Aeroelastic system development using proper orthogonal decomposition and Volterra theory, AIAA Paper 2003-1922.
Lucia, D., Beran, P., Silva, W., 2004. Reduced order modeling: new approaches for computational physics. Progression Aerospace Sciences 40, 51–117.
Mehner, J.E., Gabbay, L.D., Senturia, S.D., 2000. Computer-aided generation of nonlinear reduced-order dynamic macromodels—II: Stress-stiffened case. Journal of Microelectromechanical System 9 (2), 270–278.
Myers, R.H., Montgomery, D.C., 2002. Response Surface Methodology. Wiley, New York.
Romanowski, M., 1996. Reduced order unsteady aerodynamic and aeroelastic models using Karhunen-Loève eigenmodes, AIAA Paper 96-3981.
Silva, W., 1997. Identification of linear and nonlinear aerodynamic impulse responses using digital filter techniques, AIAA Paper 1997-3712.
Silva, W., 1999. Reduced order models based on linear and nonlinear aerodynamic impulse response, AIAA Paper 1999-1262.
Silva, W., Bartels, R.E., 2002. Development of reduced-order models for aeroelastic analysis and flutter prediction using the CFL3Dv6.0 Code, AIAA Paper 2002-1596.
Silva, W.A., Reveh, D.E., 2001. Development of unsteady aerodynamic state-space models from CFD-based unsteady loads, AIAA Paper 2001-1213.
Tang, D., Dowell, E., Hall, K., 1999. Limit cycle oscillations of a cantilevered wing in low subsonic flow. AIAA Journal 37 (3), 364–371.
Tang, D., Kholodar, D., Juang, J.-N., Dowell, E., 2001. System identification and proper orthogonal decomposition method applied to unsteady aerodynamics. AIAA Journal 39 (8), 1569–1576.
Thomas, J., Dowell, E., Hall, K., 2002. Nonlinear inviscid aerodynamic effects on transonic divergence, flutter and limit cycle oscillations. AIAA Journal 40 (2), 638–646.
Thomas, J.P., Dowell, E.H., Hall, K.C., Denegri, C.M., 2004. Modeling limit cycle oscillation behavior of the F-16 Fighter using a harmonic balance approach, AIAA Paper 2004-1696.